SURFACE TEMPERATURE VARIATIONS DURING THE LUNAR NIGHTTIME*

BRUCE C. MURRAY AND ROBERT L. WILDEY
Division of Geological Sciences, California Institute of Technology, Pasadena, California
Received May 23, 1963; revised October 3, 1963

ABSTRACT

A new photometer incorporating a mercury-doped germanium photoconductor has been used with a 19-inch telescope to measure the 8–14-μ brightness temperatures of the shaded lunar surface. Right-ascension scans carried into the lunar nighttime from the terminator show a characteristic pattern of cooling inconsistent with the occurrence of a thick homogeneous dust layer. It appears that more highly conducting material either is exposed commonly on the surface or constitutes a substratum generally covered by no more than a centimeter or so of the strongly insulating dust. No difference in nighttime temperature distribution was observed between maria and uplands. However, local areas of higher-than-average brightness temperature were encountered. These indicate extensive exposures of consolidated material. Local temperature anomalies of this type are associated with the bright-rayed craters Tycho and Copernicus, but they are distributed over an area larger than that represented by the respective craters. Two other groups of temperature anomalies were found in otherwise undistinguished mare border areas.

These observations and others suggest that surface redistribution processes are operative on the lunar surface over at least a 10-meter range, but are not important over distances much in excess of a kilometer.

I. INTRODUCTION

During 1961, an effort was initiated at the California Institute of Technology to exploit, for astronomical purposes, the high instrumental sensitivity of newly developed photoconductive detectors at wavelengths out to 14 μ and beyond. Murray and Wildey (1963) have given a preliminary report of observations during the first 160 hours of the lunar nighttime at wavelengths from 8 to 14 μ. In the present paper those observations are described in full, and additional evidence is presented for horizontal and vertical variations in thermal properties of the lunar surface materials. Earlier work in these wavelength ranges goes back to Rosse (1869) and Very (1898); important recent contributions include those of Shorthill, Borough, and Conley (1960) and of Sinton (1960*a*), in addition to the fundamental work of Pettit and Nicholson (1930).

II. COLLECTION AND REDUCTION OF OBSERVATIONS

a) Equipment and Site

The equipment and site used for the lunar observations are described in detail by Westphal, Murray, and Martz (1963). The detector is a mercury-doped germanium photoconductive cell[1] at the apex of a conical cavity which is maintained at liquid-hydrogen temperature ($\sim$20° K). An f/15 beam of radiation from the primary mirror is directed into the cold cavity by a barium fluoride Fabry lens. An interference filter within the cavity, combined with the sensitivity function of the cell, restricts the effective pass band to the interval 8-14 μ, as shown in Figure 1. The doped-germanium photoconductor mounted in this fashion has a noise-equivalent power approaching 2×10^{-12} W, that is, about 100 times smaller than that of a good thermal detector operated at ambient temperature. Further refinement of equipment eventually may lead to a noise-equivalent power approaching 10^{-14} W.

In front of the cold cavity is a focal plane diaphragm. A 0.6-mm aperture was used

* *Contribution of the Division of Geological Sciences, California Institute of Technology*, No 1173, Pasadena, California.

[1] Manufactured by Texas Instruments, Inc.

for the lunar observations, corresponding to 17 sec of arc at the focal length used. The image is, in effect, switched by a dual-beam photometer (Fig. 2) at 180 cps from that of a small portion of the lunar surface to that of an equal angular area of sky beside the moon and back again. The switching is closely "square wave" and does not involve any image motion. The alternation in total incident 8–14-μ radiation between the two halves of the switching cycle generates a small phased-locked square-wave voltage fluctuation; this is amplified, synchronously rectified, and recorded on a strip-chart recorder. The spectral response of the system is constant and known and the photoconductive cell is not known to depart from a constant monochromatic responsivity within the intensity range of the present observations. Hence, the deflection on the strip-chart recorder can be directly related to the intensity of the lunar radiation in the 8–14-μ interval, reduced by atmospheric and telescope transmission losses.

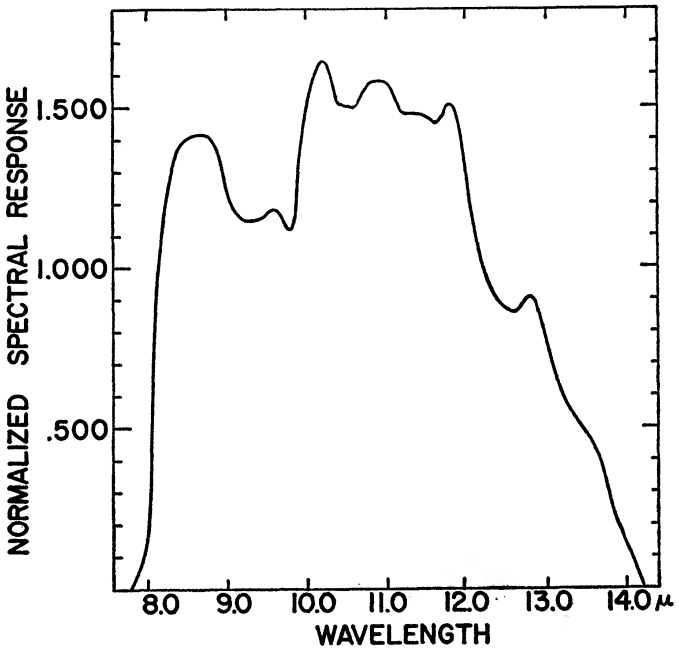

FIG. 1.—Spectral response of the photometer normalized to mean value of unity over the range of 8–14 μ. Original measurements were obtained through the courtesy of the Naval Ordnance Research Laboratories, Corona, California.

The photometer was used at the $f/15$ Cassegrain focus of a portable 19-inch telescope designed especially for lunar infrared observation. The $f/2$ primary was made available by the Mount Wilson and Palomar Observatories. All mirrors were gold-surfaced because published data (Allen 1955; Harris and Fowler 1961) indicate that gold-surfaced mirrors should be superior to aluminum-surfaced ones in the 8–14-μ region. The telescope was located in a small prefabricated dome at an elevation of 3880 m on White Mountain, California, at $\lambda = 118°$ W., $\phi = +37°.5$. Lunar observations discussed in this paper were collected there during August and September of 1962.

b) Formal Relationships and Calibration Procedure

Let D be the deflection in volts on the strip-chart recorder; G the electronic gain through a linear electronic system; and V_0 the average a.c. output voltage of the cell during the integration time of electronics and recorder, between 0.1 and 1.0 sec. Then,

$$D = GV_0 . \quad (1)$$

The modulation is closely "square wave" and has a period of 1/180 sec. This is small compared to the electronic integration time, 1/10–1 sec, but long compared to the intrinsic time constant of the cell, 10^{-6} sec. Therefore

$$V_0 = V_{ab} + V_{cn}\,, \tag{2}$$

where V_{ab} is the a.c. output voltage of the cell due to modulated incident radiation averaged over the integration period, and V_{cn} is the average a.c. output voltage due to

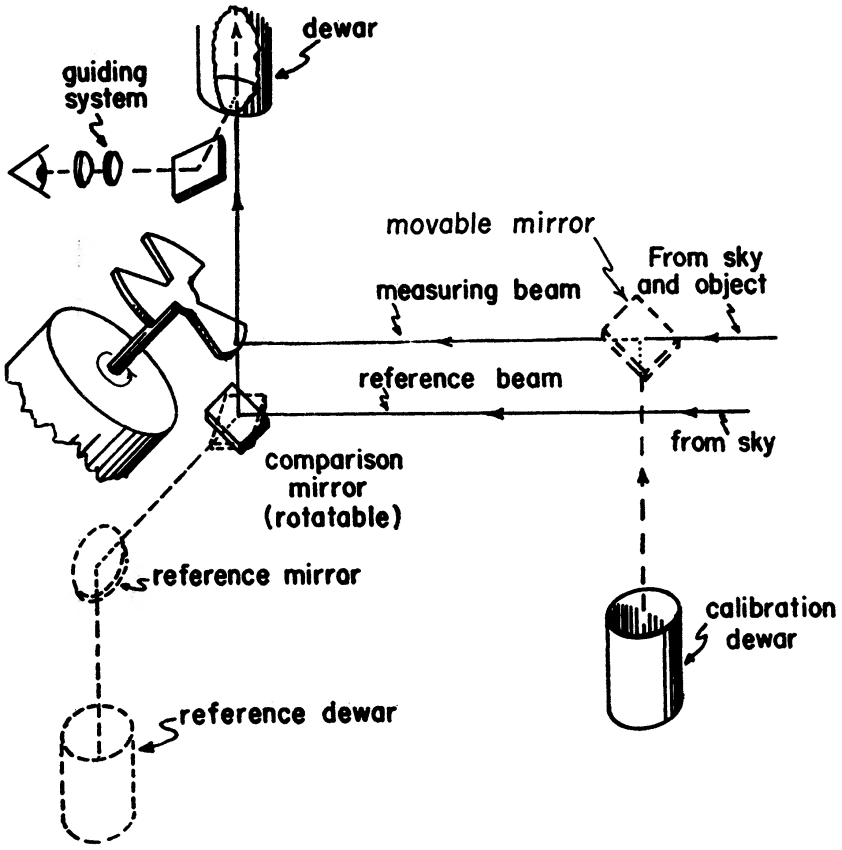

FIG. 2.—Schematic diagram of optical paths through double-beam photometer. Calibration mode indicated by dashed lines.

other sources: for example, Johnson noise, microphonic effects, current noise, etc. For the applications of this paper, $V_{cn} \ll V_{ab}$ and will not be included further. Therefore,

$$V_0 = V_{ab}\,. \tag{2a}$$

The monochromatic responsivity R_λ of photoconductive cells is a function not only of cell temperature and intrinsic cell properties but also of the "background" flux (Smith, Jones, and Chasmar 1957; Bratt, Engeler, Levenstein, MacRoe, and Perek 1961). No non-linearity has been detected over the range of background fluxes encountered in either the observational or calibration modes of the present investigation. It should be noted, however, that for the kinds of signal and background fluxes encountered in lunar observations through the telescope, direct simulation in the laboratory is beyond our present capability. Consequently, we are, in effect, extrapolating determinations of

responsivity rather than interpolating them. The relationship between incident radiation and voltage deflection is, therefore,

$$D = Gr\int_{8\mu}^{14\mu} S_\lambda [W_\lambda(A) - W_\lambda(B)]\, d\lambda\,, \tag{3}$$

where r is the 8–14-μ responsivity (a constant with units of volts/watt); S_λ is the normalized spectral response (see Fig. 1); and $W_\lambda(A)$, $W_\lambda(B)$ are the energy fluxes at the detector during the two parts of the chopping cycle. Because of non-uniformity in the sky and telescope radiation field, the integrand does not vanish even when both beams observe sky only. Let Q be the deflection that results in this use. Then

$$D = Gr\,\bar{\rho}\,A\,\Omega\int_{8\mu}^{14\mu} S_\lambda I_\lambda E_\lambda(\text{sec. } Z)\, d\lambda + Q\,. \tag{4}$$

Here A is the area of the focal plane aperture; Ω the area of the primary mirror divided by the square of the effective focal length; I_λ the monochromatic brightness of the moon; and E_λ (sec. Z) the atmospheric transmission at the zenith distance Z of observation. The coefficient $\bar{\rho}$ describes the transmission of the telescope, but not the photometer; included in it is a factor for the obscuration by the secondary mirror.

Let us suppose that $I_\lambda = B_\lambda(T_b)$, where B_λ is the Planck intensity at temperature T_b. Then one can define the quantities

$$b(T_b, \text{sec. } Z) = \int_{8\mu}^{14\mu} S_\lambda [B_\lambda(T_b) E_\lambda(\text{sec. } Z)]\, d\lambda\,, \tag{5}$$

and

$$N(T_b, \text{sec. } Z) = \frac{b(T_b, \text{sec. } Z)}{b(273^\circ\text{K}, 0)}\,. \tag{6}$$

The function $N(T_b, \text{sec. } Z)$ is shown in Figure 3 for the S_λ of Figure 1 and the atmospheric transmission model used in the reduction of the present observations (Fig. 4). The net deflection is

$$D - Q = Gr\bar{\rho}A\Omega N(T_b, \text{sec. } Z)\; b\;(273^\circ\text{ K}, 0)\,. \tag{7}$$

The calibration mode of the photometer provides a means of viewing a water-ice black-body cavity and a liquid-nitrogen black-body cavity through the same solid angle as is subtended by the primary mirror at the Fabry lens. Thus the deflection $(D - Q)$ corresponding to 273° K can be observed directly. Accordingly,

$$(D - Q)_{273^\circ\text{K}} = GrA\Omega b\;(273^\circ\text{ K})\,, \tag{8}$$

and therefore

$$N(T_b, \text{sec. } Z) = \frac{1}{\bar{\rho}}\,\frac{D-Q}{(D-Q)_{273^\circ\text{K}}}\,. \tag{9}$$

This equation gives N $(T_b, \text{sec. } Z)$ in terms of observable or known quantities, and Figure 3, the calibration curve, relates the $N(T_b, \text{sec. } Z)$ to the 8–14-μ lunar-brightness temperature.

c) Transmission Losses and Estimates of Accuracy

The spectral transmission of the atmosphere in the 8–14-μ region has been the subject of both theoretical and observational investigation for many years. However, neither the dependence of extinction on zenith distance nor the temporal variation of extinction to be expected is firmly established at the present time. Furthermore, the reflectivity of our gold-surfaced mirrors appears to be appreciably lower than the 99 per cent suggested by published data (Harris and Fowler 1961). It would be desirable to control

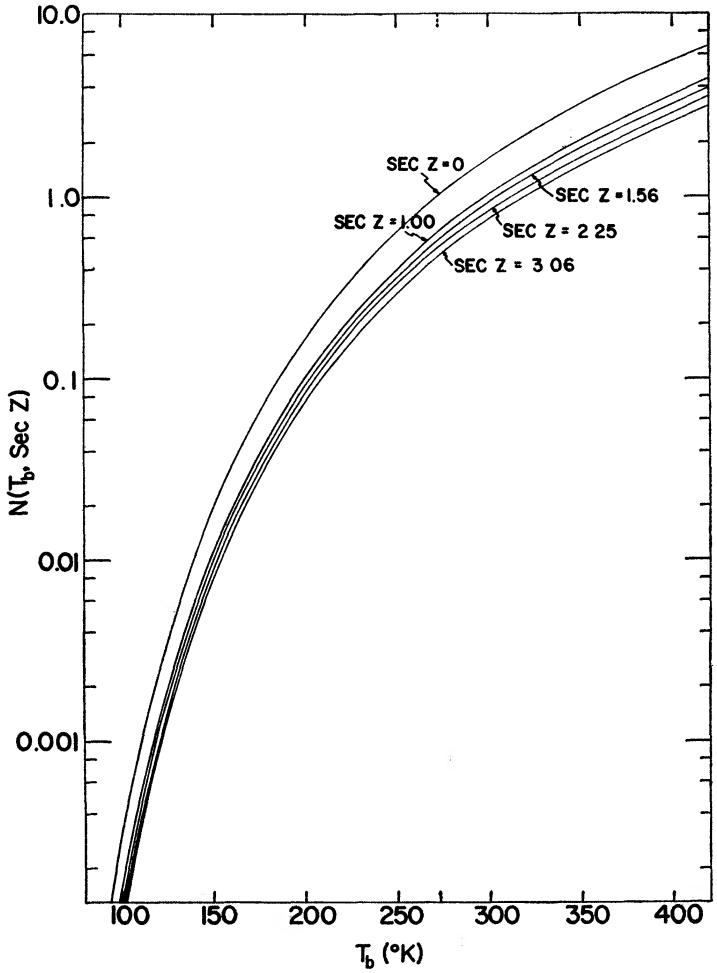

FIG. 3.—Calculated response of photometer to radiation from extended objects outside atmosphere Atmospheric transmission losses for various path lengths are also included. The response has been normalized to that for 273° K and no atmospheric transmission losses.

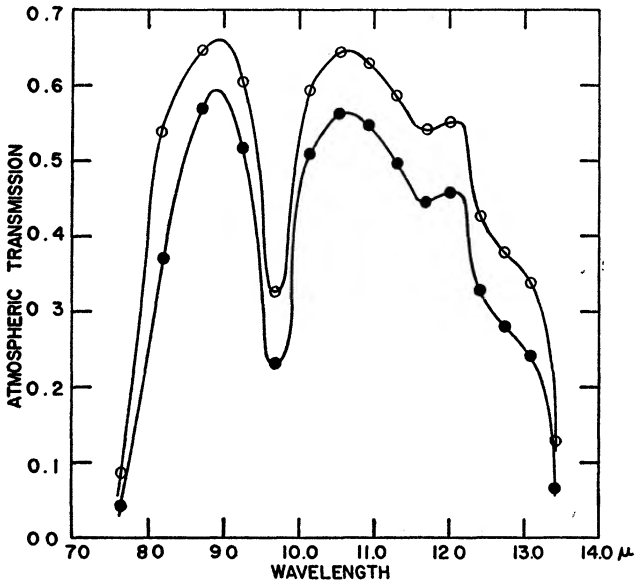

FIG. 4.—Atmospheric spectral transmission for 2.25 air masses. The closed circles are the results of Sinton and Strong (1960 *a*, *b*) for Palomar Mountain, and the open circles are those assumed in the present paper for White Mountain.

such transmission losses by nightly observations of "standard" planetary or stellar objects. Unfortunately, only one possible "standard" object (Jupiter) was accessible to our 19-inch telescope at White Mountain and there is no independent knowledge of the actual 8–14-μ brightness temperature of Jupiter. Accordingly, a modified form of the extinction model of Sinton and Strong (1960*a*, *b*) was used. Despite the limitation of being able to observe only one "standard" celestial object, the repeated observations of Jupiter over a moderate range of secant zenith distance provide a measure of the nightly variability of combined extinction and calibration errors, as well as a means of detecting any gross systematic error in extinction.

The Sinton and Strong extinction model utilizes a square-root dependence on the secant zenith distance. The spectral distribution of atmospheric transmission measured at Palomar Mountain (elevation 1745 m) for sec. $Z = 2.25$ is shown as the lower curve in Figure 4. In order to apply their results to the White Mountain site we have applied the simplified[2] transformation

$$\ln\left[\frac{A_p(\lambda)}{A_w(\lambda)}\right] = \frac{P_p}{P_w},$$

where $A_p(\lambda)$, $A_w(\lambda)$ are the coefficients of atmospheric absorption at Palomar and White Mountain, respectively; and P_p, P_w are the corresponding ambient pressures.

The resulting transmission is shown as the upper curve in Figure 4 for sec. $Z = 2.25$. Extinction coefficients for the values of sec. Z have been obtained analogously and the results incorporated in the $N(T_b, \text{sec. } Z)$ curve shown in Figure 3.

The random errors introduced by using an assumed extinction model rather than an observed one can be roughly estimated from the nightly variations in the apparent brightness temperature of Jupiter. This observed variation includes a measurable change in responsivity of the cell. The observations of Jupiter for twelve different nights yield a mean value of 128° K with a standard deviation of ± 2.3° K when reduced in the same manner as were the lunar measurements. Accordingly, we take ± 3° K at 128° K to be a reasonable upper limit for the nightly random error in the lunar observations.

In addition, there are at least two obvious sources of systematic error. The first is the extrapolation to sec. $Z = 0$, which is quite sensitive to the functional form of the zenith distance dependence. The second is the real transmission loss within the telescope. In the reduced Jupiter data there is a slight trend for the apparent brightness temperature to increase with increasing sec. Z, indicating that the deflections may have been overcorrected for supposed extinction losses. This trend is eliminated, or possibly even slightly reversed, if no extinction correction at all is used. The mean value of the brightness temperature is reduced 7° K by this procedure. It seems possible that our reduced lunar values may be systematically too high by as much as 5° K, for a temperature of 128° K, because of extinction overcorrection. On the other hand, we have assumed the transmission coefficient of the telescope (including the secondary mirror) to be unity. Actually it could be no larger than about 0.94[3] even if the mirrors had the 99 per cent reflectivity indicated in the literature. Rough measurements in the laboratory of gold-surfaced mirrors similar to those on the telescope suggest a reflectivity of about 0.93, leading to an estimate of about 0.8 for $\bar{\rho}$. Such an instrumental transmission loss, not allowed for in the data reduction, leads to brightness temperatures systematically too low by 2.5° K at 128° K. The two primary sources of possible systematic error thus have a compensating effect on the reduction procedure used for the lunar observations discussed in this paper. Accordingly ± 5° K is adopted as the likely upper limit of systematic errors and ± 3° K as the likely upper limit of random night-to-night errors in the lunar observations presented here.

[2] This transformation ignores the differential effects of pressure broadening, the existence of which is implied by the square-root dependence of the law.

[3] The obscuration due to the secondary mirror is about 4 per cent.

Finally, we can consider the differential accuracy of a given scan and the minimum detectable temperature of the entire system. Examination of the actual strip-chart records reproduced in Figures 6 and 7 (see below) shows both a "white" noise originating within the cell itself and also a distinct pattern of fluctuations in the 10–100-sec. period range.

These "low-frequency" fluctuations may arise from non-stationary emission originating in the telescope and in the atmosphere as viewed by the double-beam photometer and possibly also in the instrument itself. Scan VIII is included to illustrate a night when this low-frequency noise was particularly strong. In general, the low-frequency noise was the limiting noise for the determination of temperatures on the lunar scans and resulted in a minimum detectable brightness temperature of about 105° K for a small area on the moon. Thus the differential accuracy in temperature measurement of a given scan is generally limited to a deflection reading corresponding to 105° K. In terms of signal-to-noise ratio the differential accuracy (or "reading" accuracy) in temperature is illustrated by Table 1, derived from Figure 3.

There is no electronic integration in the above data; the effective low-pass filter of the system is the recorder itself, with time constant of about $\frac{1}{4}$ sec.

TABLE 1

DIFFERENTIAL ACCURACY OF SCANS

Lunar Brightness Temperature (° K)	Approximate Signal-to-Noise Ratio	Lunar Brightness Temperature (° K)	Approximate Signal-to-Noise Ratio
105	1:1	145	24:1
115	2 5:1	155	43:1
125	6 5:1	165	69:1
135	12 5:1		

III. THE OBSERVATIONS

a) Introduction

The observations discussed in this paper were obtained on the nights of August 21/22, 23/24, and 24/25, and September 22/23, 1962. Tracings of some of the original strip-chart records are shown in Figure 6. The scan tracks of all the observations used are plotted in Figure 5. Right-ascension scans were begun just sunward of the evening terminator; carried across most, or all, of the shadowed lunar surface; and then reversed in direction until the terminator was again crossed. The reversal point was far enough from the terminator that the lunar temperature was usually below the system noise level and, hence, the reversal point could be taken to be a measurement of "sky only" to provide a zero brightness reading (Q). The reference beam of our double-beam system was always either on the sky or on a part of the dark moon far enough from the terminator to have no detectable emission. In addition, the telescope was moved off the moon before and after most of the scans to provide additional zero brightness readings. The non-coincidence of forward and reverse scans is due to the motion of the moon in declination. We were unable, therefore, to repeat the exact geographic coverage of each scan, which is one reason why the anomalous features illustrated in Figure 6 do not reproduce exactly between the left and right sides of the figure. The linear spatial resolution of the measurement, with allowance for diffraction and seeing, is 26 sec. of arc, corresponding to about 50 km at the sub-earth point of the lunar surface.

Accurate, continuous determination of position of the focal plane aperture with respect to the image of the unilluminated lunar surface is a formidable problem. The positional

information required to produce Figure 5 was obtained by taking 35-mm photographs at the beginning, reversal, and ending points of each scan through a small finder telescope fitted with a reticle. The cross hairs, which could also be observed visually through a separate eyepiece, were aligned to correspond with the photometer aperture position by setting on a small, prominent, illuminated lunar crater. Additional photographs were sometimes taken at the time of crossing a prominent temperature anomaly; these served to better pinpoint related positions. The positional errors resulting from the difficulty in reading positions accurately on such low-resolution photographs are significant, but they probably do not correspond to more than two or three times the resolution limit. In some instances, however, the setting of the finder with respect to the photometer was disturbed and a systematic shift introduced. Since additional check-photographic posi-

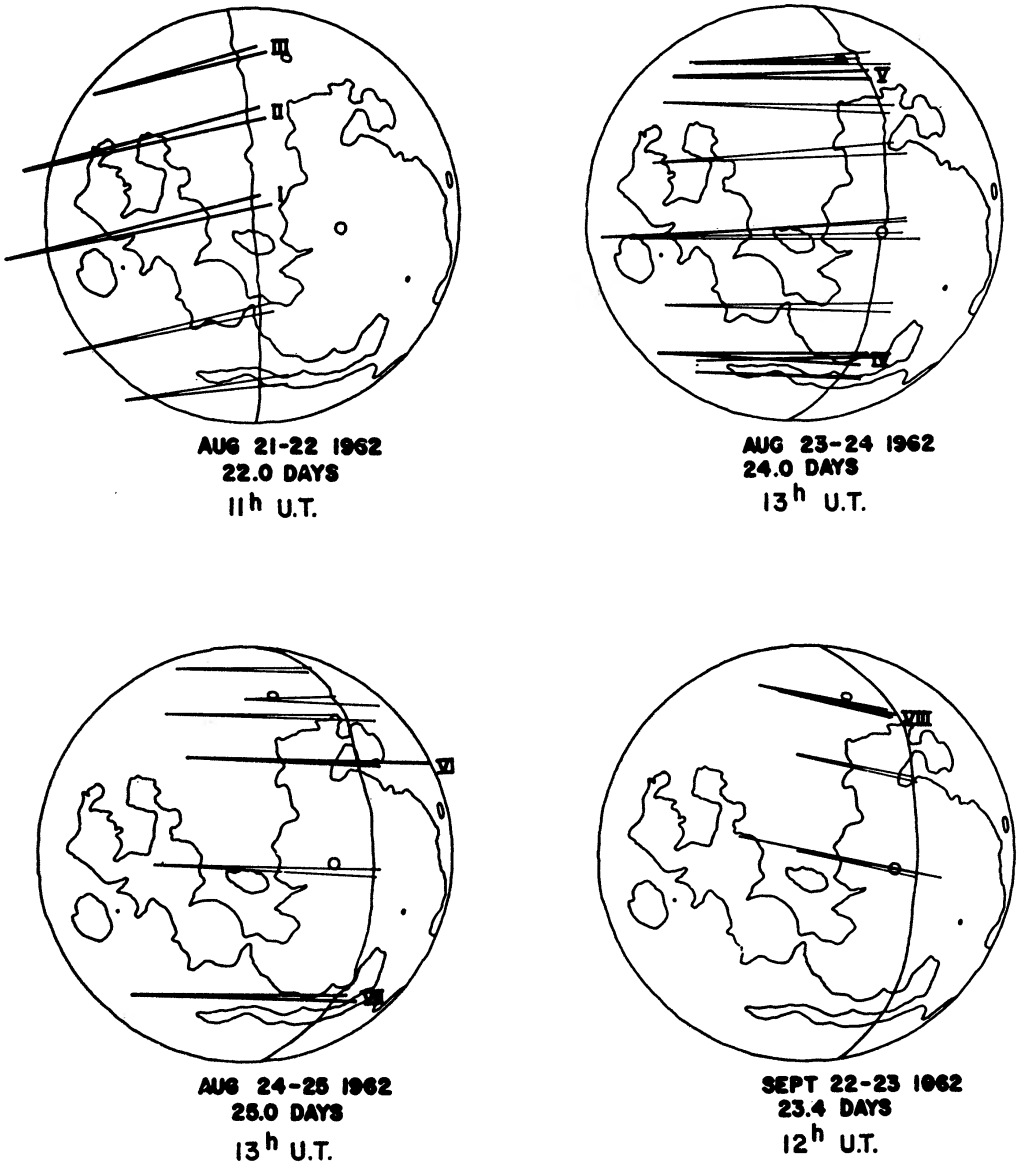

FIG. 5.—Locations of lunar right-ascension scans discussed in this paper with date and time of observations and age of moon. The systematic skewing of the scan lines between nights is an effect resulting from the variation of libration. Scans identified by a roman numeral are reproduced in Fig. 6.

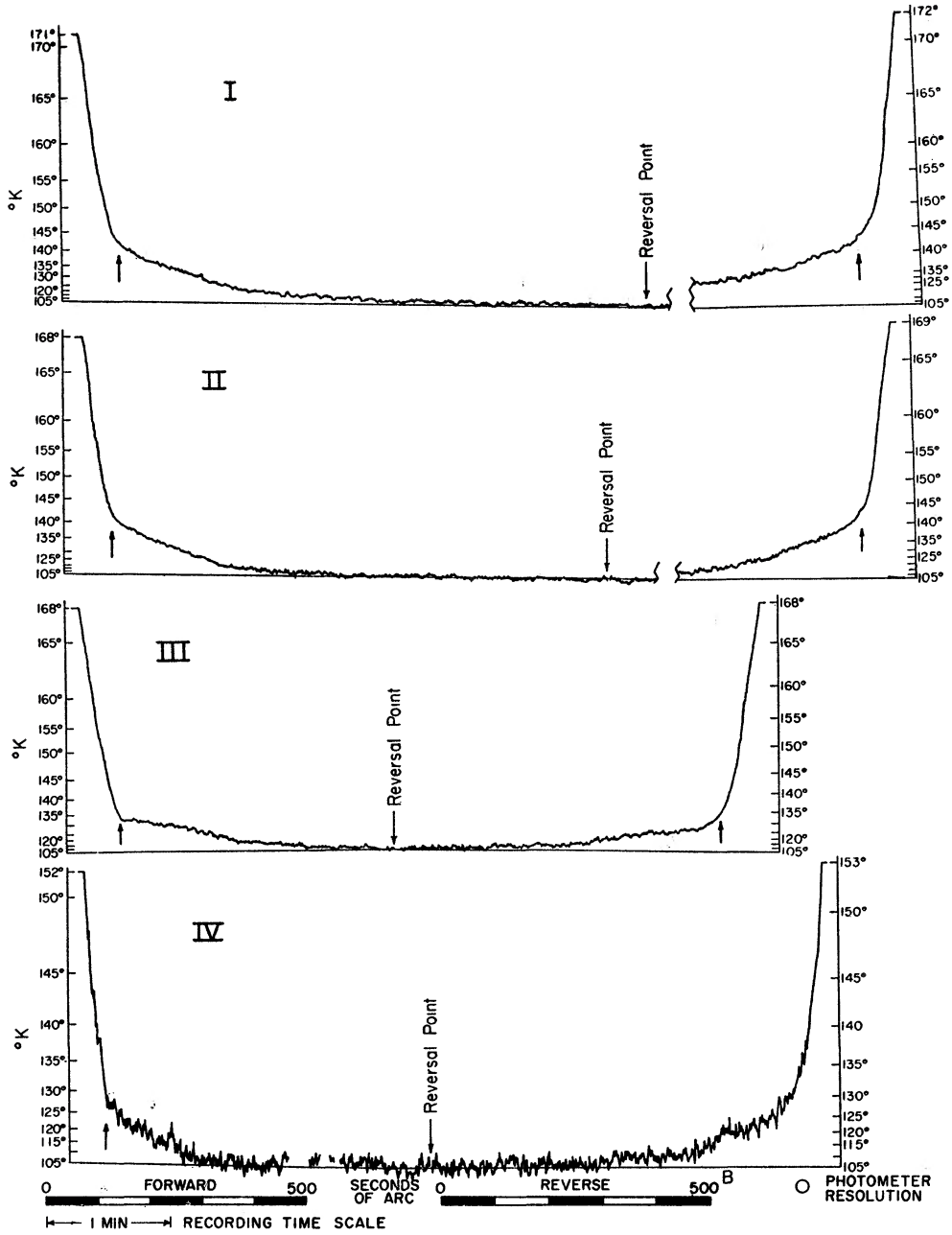

FIG. 6.—Tracings of strip-chart recordings of voltage deflection versus time for scans indexed in Fig. 5. Reduced brightness temperatures in °K are also shown in the vertical scale. Note that this scale is not the same in all scans. The time base of the recordings is shown along with a scale illustrating the angular displacement in sec of arc. The terminator, with a brightness temperature of 200° K or greater, is off scale on the tracings, but is located twice in each scan between the abscissa points at the very beginning and ending of each scan, where the recorder pen was "pegged," and the points where the deflection was a maximum and on scale.

Scans I, II, and VII have been broken in order to facilitate presentation here. The arrows near the ends of Scans I–IV, VII, and VIII denote a characteristic abrupt change in slope. *A* and *B* refer to definite and probable or possible anomalies.

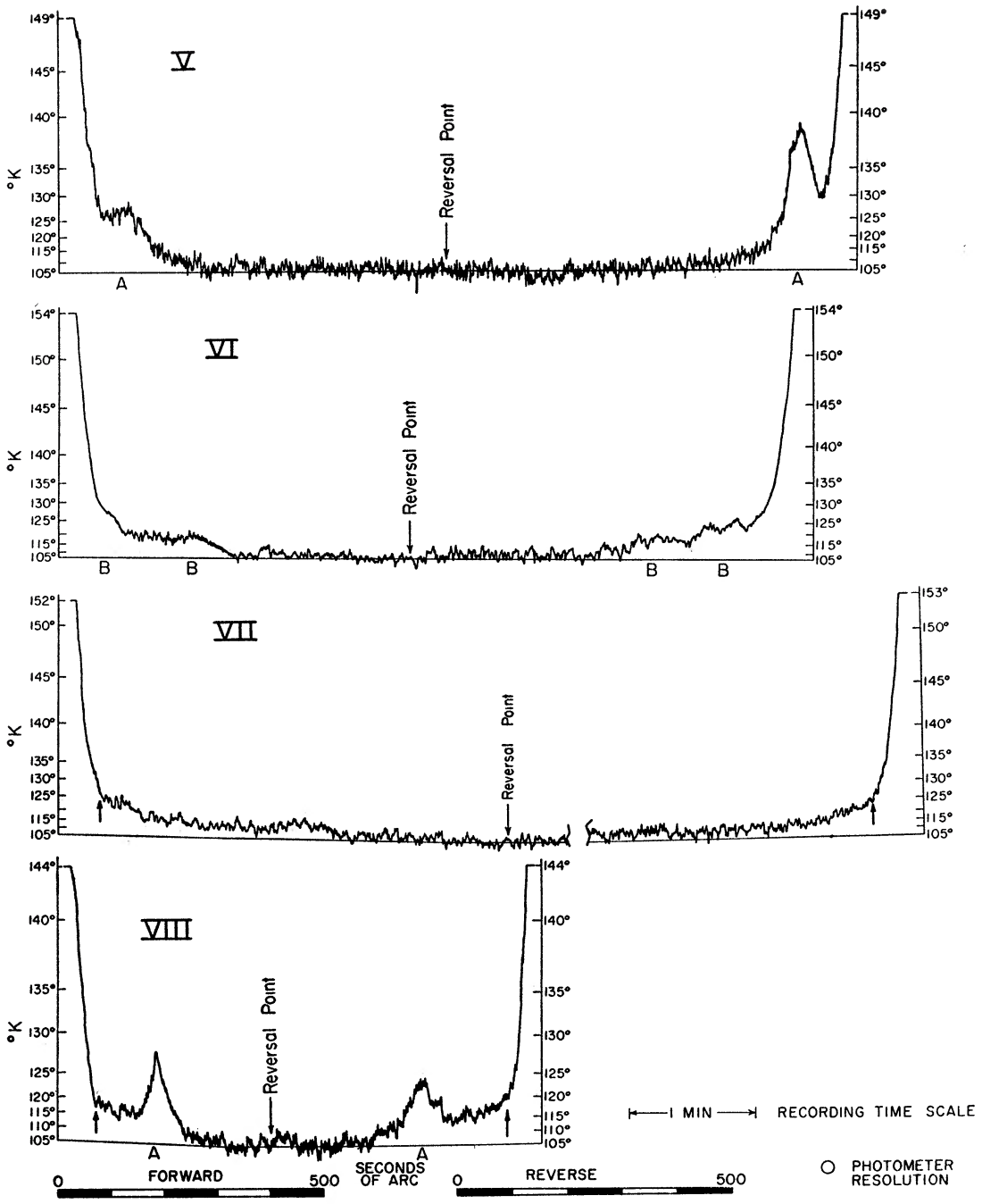

FIG. 6—*Continued*

tions were usually acquired during the run, such systematic errors could sometimes be corrected. However, systematic positional errors of perhaps five times the resolution may still persist.

b) Variation in Brightness Temperature with Selenographic Longitude

Scans I–VIII have been selected to illustrate not only typical scans but also local anomalies, the effects of poor observing conditions, and the effects of variations in latitude and phase angle. The general form of the variation of brightness temperature with longitude persists, however. It is characterized by three features: (1) a very steep gradient (perhaps even steeper than indicated because of the finite photometer resolution) in the first 6° (12 hours) or so into the lunar nighttime; (2) in most cases a rather abrupt change, in the temperature range 120°–145° K, to a more moderate slope; and (3) continued decrease in brightness temperature until the system noise level of 105° K (referred to outside the atmosphere) is reached.

In Figure 8 (see below) the forward and reverse halves of Scan I have been averaged and replotted in a linear diagram of brightness temperature versus hours since passage of the terminator. The form of the curve in Figure 8 seems to be characteristic of brightness temperature versus longitude elsewhere on the lunar surface, except that the temperature at which the gradient becomes more moderate is lower at higher latitudes and at later lunar ages, and the temperature seems to fall below the 105° K limit after a somewhat shorter duration of lunar nighttime in these cases. There also seems to be a tendency for the change in gradient to be somewhat more abrupt at higher latitudes (i.e., Scans III and VII).

c) Local Anomalies in Brightness Temperature

As is illustrated in Scans IV, V, VI, and VIII, anomalously "hot" regions occur. The term anomalous is used here in a geophysical sense, that is, to denote a local departure from a regional pattern of variation of a physical quantity. Class A anomalies, considered to be definite evidence of a local variation in surface thermal properties, are those in which a clear reversal of slope occurred on both the forward and reverse portions of the scan. Class B anomalies, regarded either as probable or possible evidences of anomalous thermal properties, include those in which only a flattening was observed instead of a clear reversal or in which the feature did not reproduce satisfactorily on both the forward and reverse parts of the scan.

The upper part of Figure 7 shows the locations of the anomalies encountered on the scans of Figure 5. The lower part of the figure is an index map. It can be seen that there are groupings of definite anomalies around Tycho and Copernicus and also Class B anomalies in two otherwise undistinguished areas along mare borders. The anomalies detected on individual scans, at least in the case of Tycho and Copernicus, are definitely part of an association of larger geographic size than either of the rayed craters in question. Also the anomalies intersected on a single scan, that is, IV, V, VI, or VIII, are generally larger than the photometer resolution, and indeed exhibit considerable structure. Thus it appears that at least Tycho and Copernicus are each associated with a complex of thermal anomalies and not just with a single anomaly identical with the crater itself. It should be noted that since there is evidence for detailed structure below the photometer resolution as well as for over-all size larger than that resolution, the apparent peak temperature encountered, for example, 138° K in Scan V, is only a lower limit for the real brightness temperature within that 50-km circular area.

A thorough search was made of the Tycho area near first quarter, that is, 10–12 days into the lunar nighttime, without any lunar radiation being detected.

The two anomalous regions in the mare border area both have a few small-rayed craters that may be associated with the anomalies; it may be that thermal anomalies are generally characteristic of bright-rayed craters.

IV. DISCUSSION

a) Introduction

In order to relate observations of lunar-brightness temperature to the physical properties of the lunar surface, departures from black-body conditions must be independently ascertained. Lunar 8–14-μ radiation was first shown to be non-Lambert in directional properties by Pettit (1935) from time-sequence observations of specific intensity at the

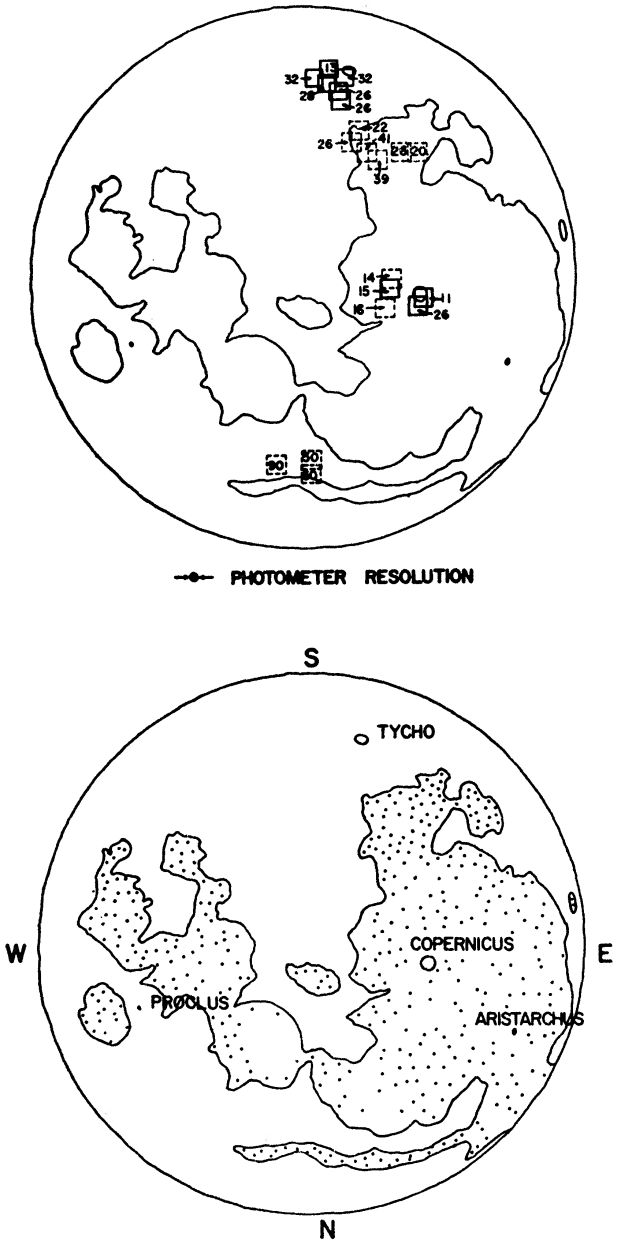

FIG. 7.—Locations of anomalies in 8–14-μ brightness temperature detected in scans shown in Fig. 5, along with lunar index map. Solid-line squares represent definite anomalies, examples of which are indicated by the symbol *A* in Fig. 6. Dashed-line squares represent probable or possible anomalies, examples of which are indicated by the symbol *B* in Fig. 6. The number inside the square is the approximate number of hours since passage of the terminator.

subsolar point. The observed limb darkening is not significant compared to likely systematic errors in flux measurements, except in extreme limb regions. In addition, possible departure from Planckian distribution was initially discussed by Pettit and Nicholson (1930) who noted that silicate slabs exhibit enhanced reflectivity—and, therefore, reduced emissivity—at certain wavelengths within the 8–14-μ region (e.g., Rubens plates). They pointed out, on the other hand, that silicate aggregates could be expected to approach unity emissivity as the grain size is decreased (a phenomenon recently documented properly by Lyon and Burns 1963). Their eclipse cooling observations strongly indicate that powdered material constitutes the very outermost surface layer of the Moon, a conclusion independently indicated also by the brightness versus phase and plane polarization observations. Accordingly, they concluded that the emissivity probably could be considered to be unity. In fact, they found it difficult to keep the observed brightness temperature at the subsolar point from exceeding that possible on the basis of solar heating and reradiation. Sinton (1960*b*) experienced similar difficulties and was led to propose occasional enhancement of solar corpuscular radiation in order to remove the apparent discrepancy. Accordingly, the lunar 8–14-μ radiation very likely is sufficiently Planckian in intensity and Lambert in directionality that the brightness temperatures discussed here can be treated as surface kinetic temperatures within the previously discussed $\pm 5°$ K (40 per cent in flux) estimated upper limit of systematic error.

It should be noted, however, that some local anomalies in brightness temperature correspond to small enough variations in 8–14-μ flux that geographical differences in 8–14-μ emissivity corresponding to differences in surface composition and/or texture must remain as a possibility. Also, finely divided silicates are partially transparent in some parts of the 8–14-μ region (Launer 1952). This fact combined with very high temperature gradients which exist in the upper submillimeter of the lunar surface may result in small, but compositionally significant, departures from Planckian distribution. Additional observational work of higher wavelength resolution will be required to investigate further these most interesting possibilities.

b) Geophysical Significance of the Longitudinal Variation of Surface Temperature

In the absence of large-scale geographic variations in thermal properties, the variation of nighttime surface temperature with longitude on the Moon can be considered to be a measure of the time variation of temperature at a single point. Indeed, the initial temperature differences arising from variations in albedo are damped out so quickly that no effect is apparent on the scans as the boundaries are crossed between mare and upland areas. Accordingly, the two halves of Scan I were averaged (to eliminate the effects of any linear error in base line) and plotted in Figure 8 as a function of time since passage of the terminator. Figure 8 thus represents the portion of the cooling curve of an "average" equatorial area on the Moon for the first 160 hours or so of the lunar nighttime. The daytime portion of the cooling curve has been measured previously (Geoffrion, Korner, and Sinton 1960; Pettit and Nicholson 1930), but the nighttime portion previously had to be estimated from the higher temperature eclipse-cooling observations. The eclipse cooling observations are only influenced by the thermal properties of the outermost millimeter or so, and they tell us little more than that this thin skin is an exceedingly good thermal insulator. The present observations extend well into the lunar nighttime and provide the first direct investigation of the thermal properties of the Moon in the depth range of a few millimeters to a few centimeters. Microwave observations have been made at wavelengths as short as 1.5 mm (Sinton 1955), but these observations probably still see "through" the layers presently being discussed. In particular, the nighttime cooling curve can provide direct evidence of vertical and horizontal inhomogeneities. The problem has been investigated theoretically (see discussion in, and references at end of, Sinton 1962); we find the analysis of Jaeger (1953) to be the most useful for purposes of qualitative comparison of our observations with simple models. He computed

both the lunation cooling curves and eclipse cooling curves for a thick layer of material with various values of $(k\rho c)^{-1/2}$, where k is the thermal conductivity, ρ the density, and c the specific heat. He found that a value of $(k\rho c)^{-1/2}$ of about 1000 in calories and cgs units best satisfied the eclipse cooling observations of Pettit and Nicholson (1930). This corresponds to a value of $k\rho c$ about 2500 times smaller than that of consolidated rock and is consistent with the concept of a porous powder constituting the very outer skin of the Moon. He also considered the case where this skin is less than 1 cm thick and is underlain by a thick layer of more conductive material with thermal properties similar to consolidated rocks. Layers substantially thicker than a few centimeters degenerate

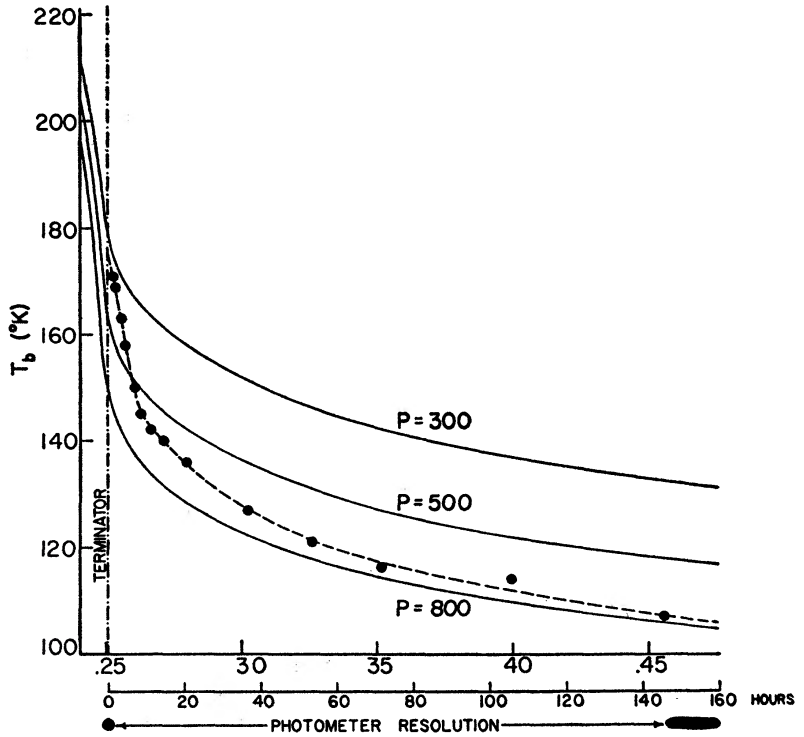

FIG. 8.—Comparison of calculated and observed lunation cooling curves. The observations of Scans I and II, August 21–22, 1962, have been averaged and plotted (*filled circles*) as a function of time since passage of terminator. Also shown are calculated lunation cooling curves for an arbitrarily thick surface layer of $(k\rho c)^{-1/2}$ of 300, 500, and 800. The calculations are after Jaeger (1953), but are considerably more precise than those in his paper. An albedo of 20 per cent was assumed. The thermal properties were assumed to be independent of temperature in Jaeger's analysis.

into a single-layer case. In all his calculations he considered the thermal conductivity to be constant within each layer, recognizing, however, that a temperature-dependent conductivity might actually occur. Without specific information on such a dependence, more refined calculations provide little additional enlightenment.

Three of Jaeger's curves have been recomputed using 400 points per lunation rather than the 20 he used. They are reproduced in Figure 8 for comparison. It is clear that none of the curves fits at all well. It may not even be possible to explain by simple theory the observed curve with any kind of layering. In any case, a homogeneous layer of porous dust of centimeters-to-meters thickness is clearly ruled out.

An alternative is that horizontal variations in conductivity arise from bare outcrop or boulders on the surface. Such a configuration could probably produce at least as good a fit as can the vertical variation model, without exceeding the 10 per cent limit to the

areal extent of meter-wavelength scattering material imposed by radar observations (Evans 1962). In any case, it can be concluded that conductive material must either be exposed at the surface or within a few centimeters of it over most of the Moon. In particular there appears to be no difference between mare and upland areas in this regard. This is a result of considerable importance to theories of dust on the Moon, since it would now seem possible for there to be significant amounts of porous dust *only* if this is mixed uniformly with blocks of consolidated rocks—that is, resembling a breccia. Such a deposit might well characterize the lunar surface if an equilibrium exists there between rock-consolidation processes and rock-degradation processes (i.e., impact).

c) Geological Implications of Local Temperature Anomalies

The local departures from the general pattern of longitude-dependent cooling are all positive; this suggests local exposures of more conductive surface materials. Natural heat sources appear to be ruled out as a cause of the local anomalies because of the enormous power requirements to maintain such large surface-temperature differences over tens or hundreds of square kilometers. Also, the Tycho anomalies, at least, appear to disappear during the nighttime, as would be expected of diurnal heating and cooling. Near Tycho and Copernicus, these anomalous surface deposits appear to be distributed somewhat irregularly over an area considerably larger than the rayed crater itself. These same rayed craters display a *lower* daytime temperature—due to higher albedo—than do the surrounding areas (Shorthill and Saari 1961); hence the anomalous nighttime temperatures cannot result from differences in total absorbed daytime solar radiation.

It is clear that a significant fraction of the surface within and about these two most prominent, and very probably "recent," lunar impact craters is not covered with the same amount of the highly insulating dust which characterizes the great proportion of the lunar surface. Probably, however, at least a very thin veneer of dust is still present; otherwise, corresponding anomalies would occur in visible polarization (Dollfus 1962) and brightness variation with phase (Van Diggelen 1960; Wildey and Pohn 1963). Hence, it seems likely that the conductive material is covered by only a thin layer, perhaps less than 1 mm in thickness, of the highly insulating dust. The anomalies suggest either nearly bare consolidated rock outcrop (including in this term compacted and cemented dust, or dust and impact debris, as well as crystalline rock or possibly a dense distribution of large blocks. Secondary impact craters clustered about the primary craters should provide considerable exposures of such consolidated rock also. A very rough surface on the meter scale in the vicinity of Tycho is strongly suggested quite independently by the radar observations of Pettengill and Henry (1962), even though, on the average, the lunar surface is quite smooth at radar wavelengths (Evans 1962).

All of this adds up to a picture not at all incompatible with some of the geological details expected by Shoemaker (1962) and others to characterize large impact structures on the Moon. However, some interesting questions arise in connection with the geological processes that transform this rough landscape of virtually unaltered rock surfaces into the very smooth, insulated, and darker landscape which characterizes most of the other, presumably more aged, lunar craters. Radiation damage may well provide the explanation of the darkening; but what transforms the surface from rough to smooth on a meter scale, and how do the fresh rock surfaces become covered with insulating material?

Clearly a redistribution process operating over at least 10-meter ranges must characterize the lunar surface. Gold (1955) has suggested that dust sedimentation is going on and the rough, fresh, structures are simply buried in the course of time. But, as was discussed in the preceding section, the longitudinal temperature variations observed do not seem to be compatible with a widespread unconsolidated dust layer thick enough to bury the meter-scale roughness constituting the surface of structures with kilometer-

scale relief. Furthermore, the source of this hypothetical dust sedimentation remains in doubt. Cosmic infall does not seem to be sufficient and may well actually result in greater erosion than sedimentation (Shoemaker, private communication). If the source is thought to be the Moon itself, then there should be bare, elevated areas providing the sediment to fill in the newly formed impact craters. Such bare surfaces would appear as large "hot" regions during the lunar nighttime; but it is clear that no such bare areas exist.

There are, in addition, other very serious difficulties to both the cosmic infall notion and the concept of lunar sedimentation involving transportation over distances of tens of kilometers. In particular, the distinct pattern of albedo variation in the maria and the small, but apparently real, color differences (Coyne 1963) very likely reflect local differences in underlying rock. Such variations in surface deposits would be obliterated by any large-scale redistribution of surface material.

Many of these difficulties can be avoided if the weathering, erosion, and sedimentation processes are supposed to have taken place *in situ*, with no redistribution over distances greater than, say, about 1 km.

V. CONCLUSIONS

1. The general variation with longitude of nighttime surface temperature on the Moon is incompatible with a thick uniform dust layer at the surface, of the kind that might originate by cosmic infall, for example. Conductive material apparently is commonly present either on the surface or within a few centimeters of it.

2. No nighttime temperature difference occurs between mare and upland areas; the thermal properties are apparently independent of the major physiographic characteristics of the Moon. This fact appears to rule out any significant net mass transport, in the form of fine particles, from the uplands to the maria.

3. Locally there are extensive areas of more conductive materials overlain by not more than a few millimeters of dust. Two such regions are associated with, but are larger than, the rayed craters Tycho and Copernicus. Two other, less prominent, regions on mare border areas may—or may not—be related to small rayed craters.

4. The aging process of the rayed craters involves not only darkening but a change from conducting to insulating surface conditions. According to the radar observations of Pettengill and Henry (1962), aging also produces a change from a very rough surface to a smooth one on a meter scale. Although the visual darkening effect might be dismissed simply as a radiation-damage phenomenon, the smoothing and insulation effects require weathering, erosion, transport, and sedimentation processes to occur on the present lunar surface over a range of at least 10 m.

5. The geological processes which transform rough and conductive terrain to smooth and insulating terrain must be of small scale in order to be consistent with other physical observations, probably less than 1 km in range and possibly very much less. Accordingly, the redistribution processes appear to be bracketed in the 0.01–1-km range.

The authors have received important assistance from the Mount Wilson and Palomar Observatories, from the Naval Ordnance Test Station, China Lake, California, and from the White Mountain Research Station of the University of California. We are particularly indebted to Mr. James A. Westphal, senior engineer in the Division of Geological Sciences, for the development of the photometer and other equipment and for considerable help in both the collection and interpretation of the observations. Financial support for the research described here was made available under National Aeronautics and Space Administration grant NsG56-60 and the National Science Foundation grant G25210.

REFERENCES

Allen, C. W. 1963, *Astrophysical Quantities* (London: Athlone Press).
Bratt, P., Engeler, W., Levinstein, H., MacRoe, A., and Perek, J. 1961, *Infrared Phys.*, **1**, 27.
Coyne, C. V. 1963, *A.J.*, **68**, 49.
Dollfus, A. 1962, in *Physics and Astronomy of the Moon*, ed. Z. Kopal (New York: Academic Press), p. 131.
Evans, J. V. 1962, in *Physics and Astronomy of the Moon*, ed. Z. Kopal (New York: Academic Press), p. 429.
Geoffrion, A., Korner, M., and Sinton, W. M. 1960, *Lowell Obs. Bull.*, **5**, 1.
Gold, T. 1955, *M.N.*, **115**, 585.
Harris, L., and Fowler, P. 1961, *J. Opt. Soc. Amer.*, **51**, 164.
Jaeger, J. C. 1953, *Aust. J. Phys.*, **6**, 10.
Launer, P. 1952, *Amer. Mineralog.*, Vol. **37**.
Lyon, R., and Burns, E. A. 1963, *Econ. Geology*, **58**, 274.
Murray, B. C., and Wildey, R. L. 1963, *Ap. J.*, **137**, 692.
Pettengill, G. H., and Henry, J. C. 1962, *J. Geophys. Res.*, **67**, No. 12, 488.
Pettit, E. 1935, *Ap. J.*, **81**, 17.
Pettit, E., and Nicholson, S. B. 1930, *Ap. J.*, **71**, 100.
Rosse, Lord. 1869, *Proc. R. Soc. London*, **17**, 436.
Shoemaker, E. M. 1962, in *Physics and Astronomy of the Moon*, ed. Z. Kopal (New York: Academic Press), p. 283.
Shorthill, R. W., Borough, H. C., and Conley, J. M. 1960, *Pub. A.S.P.*, **77**, 481.
Shorthill, R. W., and Saari, J. M. 1961, *Pub. A.S.P.*, **73**, 335 (abs.).
Sinton, W. M. 1955, *J. Opt. Soc. Amer.*, **45**, 975.
———. 1960*a*, *Lowell Obs. Bull.*, **5**, 23.
———. 1960*b*, *Pub. A.S.P.*, **72**, 362 (abs.).
———. 1962, in *Physics and Astronomy of the Moon*, ed. Z. Kopal (New York: Academic Press), p. 407.
Sinton, W. M., and Strong, J. 1960*a*, *Ap. J.*, **131**, 472.
———. 1960*b*, *ibid.*, p. 459.
Smith, R. A., Jones, F. E., and Chasmar, R. P. 1957, *The Detection and Measurement of Infrared Radiation* (Oxford: Clarendon Press).
Van Diggelen, J. 1960, *Rech. astr. Obs. Utrecht*, **14**, 114.
Very, F. W. 1898, *Ap. J.*, **8**, 199.
Westphal, J. A., Murray, B. C., and Martz, D. E. 1963, *Applied Optics*, **2**, 749.
Wildey, R. L., and Pohn, H. 1963, "Photoelectric Investigation of Lunar Brightness vs. Phase," in preparation.